ARCHITECTURE CIVIL ENGINEERING ENVIRONMENT
The Silesian University of Technology No. 3/2011

MODELLING STRAINS OF CONCRETE EXPOSED TO ALKALI-SILICA REACTION IN VARIABLE HYGRO-THERMAL CONDITIONS

Dariusz GAWIN [a], Mateusz WYRZYKOWSKI [b], Witold GRYMIN [c], Francesco PESAVENTO [d]

[a] Prof.; Department of Building Physics and Building Materials, Technical University of Łódź, Poland
E-mail address: *gawindar@p.lodz.pl*

[b] Dr.; Department of Building Physics and Building Materials, Technical University of Łódź, Poland
E-mail address: *mateusz.wyrzykowski@p.lodz.pl*

[c] PhD student; Department of Building Physics and Building Materials, Technical University of Łódź, Poland
E-mail address: *witold.grymin@p.lodz.pl*

[d] Prof.; Department of Structural and Transportation Engineering, University of Padova, Italy
E-mail address: *pesa@dic.unipd.it*

Received: 7.08.2011; Revised: 30.08.2011; Accepted: 26.09.2011

Abstract

A mathematical model of combined action of hygro-thermal, chemical and mechanical loads is proposed to describe chemical degradation of concrete due to ASR. The model is based on mechanics of multiphase reactive porous media. The mass-, energy- and momentum balance equations, as well as constitutive and physical relationships necessary for modelling the ASR in variable environmental conditions, are presented. A method for their numerical solution with the finite element and finite differences methods is described. The proposed mathematical model is validated by comparing the simulation results with some published experimental data concerning hygro-thermal processes and ASR expansion of concrete specimens in different hygro-thermal conditions, both constant and variable in time.

Streszczenie

Zaproponowano model matematyczny równoczesnego oddziaływania czynników cieplno-wilgotnościowych, chemicznych i mechanicznych do opisu degradacji chemicznej betonu, wywołanej reakcją alkalia-krzemionka. Model ten bazuje na mechanice wielofazowych reaktywnych ośrodków porowatych. Przedstawiono równania bilansu masy, energii i pędu oraz związki konstytutywne i fizyczne, które są niezbędne do modelowania przebiegu reakcji alkalia-krzemionka w zmiennych warunkach środowiskowych. Opisano metodę numerycznego rozwiązania równań modelu za pomocą metod różnic skończonych i elementu skończonego. Zaproponowany model matematyczny został zwalidowany przez porównanie wyników symulacji komputerowych z opublikowanymi danymi doświadczalnymi, które dotyczą przebiegu procesów cieplno-wilgotnościowych i pęcznienia próbek betonowych w różnych warunkach higro-termicznych, zarówno stałych, jak i zmiennych w czasie.

Keywords: **Alkali-silica reaction; Cement based materials; Chemical degradation; Hygro-thermal phenomena; Porous media mechanics.**

1. INTRODUCTION

Alkali-silica reaction (ASR), which is the most common form of alkali-aggregate reaction (AAR), is caused by the reaction between the reactive forms of silica in the aggregate and ions from the alkaline solution. Assuming appropriate conditions for the reaction development (high alkali content in the cement, availability of siliceous materials in aggregates and sufficient water content) an amorphous gel is created in the material pores. In presence of water the gel swells and, after filling up the pores, it induces additional stress in the skeleton.

The first notice about ASR dates back to November 1940, when Stanton, while analysing cracking of structures in Monterey County, suggested reaction occurring between alkalis in cement and silica in aggregates to be a reason of the deterioration. Henceforth many research studies have been conducted in order to get a better understanding of this phenomenon, being highly influenced by hygral and thermal conditions [1, 2, 3], as well as by the stress state [4]. Then, ASR causes a significant material deterioration [5], influencing the material transport properties [6] and strains induced by the reaction [4]. In the present work a novel mathematical model describing the ASR evolution, as well as the resulting strains and material degradation in variable hygro-thermal conditions, is proposed. The model is based on mechanics of multiphase porous media and its equations are solved numerically with finite element method. The results of some published experimental studies, concerning the ASR strains evolution, are compared with the numerical solution to validate the proposed model.

2. MATHEMATICAL MODEL

The balance equations are written by considering multiphase nature of cement based materials, which are assumed to be in hygro-thermal equilibrium state locally. The solid skeleton voids are filled partly by liquid water and partly by a gas phase. The liquid phase consists of physically bound water (which is present in the whole range of moisture content) and capillary water, which appears when the degree of water saturation exceeds the upper limit of the hygroscopic region. The gas phase in the whole temperature range is a mixture of dry air and water vapour, which is a condensable gas constituent.

The present model is an extension of the previous hygro-thermo-chemical model of concrete at early ages and beyond [7]. For the sake of brevity, only the final form of the model equations is given here. The full development of the model equations is presented in [8].

In the following, subscripts mean physical quantities related to the whole volume of medium and superscript their intrinsic values related to a single phase or constituent only. By constituent we indicate a matter which is uniform throughout in chemical composition, while phase means here different physical state of a matter (solid, liquid or gaseous). Symbols s, w, g, gw and ga denote solid skeleton, liquid water, gas phase in general, vapour and dry air, respectively. The solid phase is assumed to be in contact with all fluids in the pores.

2.1. Governing equations

The small deformation theory is assumed. The governing equations, written at macroscopic level in terms of the primary variables, i.e. gas pressure, capillary pressure, temperature and displacement vector (p^g, p^c, T, $\mathbf{u}$), take the following form:

– *Dry air mass balance equation* (including the solid skeleton mass balance) takes into account both diffusive and advective air flow, as well as variations of solid density caused by ASR and deformations of the skeleton. It has the following form [7]:

$$\frac{S_g n}{\rho^{ga}}\frac{\partial \rho^{ga}}{\partial t} - \beta_s(\alpha - n) S_g \frac{\partial T}{\partial t} + \frac{1-n}{\rho^s} S_g \left(\frac{\partial \rho^s}{\partial \varepsilon_{ASR}^{vol}} \frac{\partial \varepsilon_{ASR}^{vol}}{\partial t} + \frac{\partial \rho^s}{\partial m_{ASR}} \frac{\dot{m}_{ASR}}{\partial t} \right) - n \frac{\partial S_w}{\partial t} + \alpha S_g div\, \mathbf{v}^s + \frac{1}{\rho^{ga}} div\, \mathbf{J}_g^{ga} + \frac{1}{\rho^{ga}} div\left(n S_g \rho^{ga} \mathbf{v}^{gs} \right) = \frac{\dot{m}_{ASR}}{\rho^s} S_g. \quad (1)$$

where n is porosity, S_w and $S_g = (1 - S_w)$ are the water and the gas saturation degree, β_s is the thermal expansion coefficient of the solid phase, α the Biot coefficient, T the temperature, $\mathbf{v}^s$ the velocity of solid skeleton, $\mathbf{v}^{gs}$ the relative velocity of gas phase respect to the skeleton, ρ^{ga} and ρ^s the dry air and the solid skeleton density, $\dot{m}_{ASR}$ the skeleton mass source due to alkali-silica reaction and $\mathbf{J}_g^{ga}$ the diffusive flux of dry air.

– *Water species* (liquid + vapour) *mass balance equation* (including the solid skeleton mass balance) considers diffusive and advective flow of water vapour, mass sources related to ASR and to phase changes of vapour (evaporation / condensation and physical adsorption / desorption), and variations of solid density caused by ASR and deformations of the skeleton, resulting in the following equation [7]:

$$S_g n \frac{\partial \rho^{gw}}{\partial t} - \beta_{swg} \frac{\partial T}{\partial t} - n\left(\rho^{gw} - \rho^w \right) \frac{\partial S_w}{\partial t} + div\, \mathbf{J}_g^{gw} + div\left(n S_w \rho^w \mathbf{v}^{ws} \right) + div\left(n S_g \rho^{gw} \mathbf{v}^{gs} \right) + \frac{1-n}{\rho^s} \left(S_g \rho^{gw} + S_w \rho^w \right) \left(\frac{\partial \rho^s}{\partial \varepsilon_{ASR}^{vol}} \frac{\partial \varepsilon_{ASR}^{vol}}{\partial t} + \frac{\partial \rho^s}{\partial m_{ASR}} \dot{m}_{ASR} \right) + \alpha \left(S_w \rho^w + S_g \rho^{gw} \right) div\, \bar{\mathbf{v}}^s = -\dot{m}_{ASR} + \frac{\dot{m}_{ASR}}{\rho^s} \left(\rho^{gw} S_g + \rho^w S_w \right), \quad (2)$$

where ρ^w and ρ^{gw} are the liquid water and water vapour densities, $\mathbf{v}^{ws}$ and $\mathbf{v}^{gs}$ the water and the gas relative velocities respect to the skeleton, $\mathbf{J}_g^{gw}$ the water vapour diffusive flux and β_{swg} the thermal expansion coefficient of the multiphase system, given by [7]:

$$\beta_{swg} = \beta_s(\alpha - n)\left(S_g\rho^{gw} + S_w\rho^w\right) + n\beta_w S_w\rho^w, \quad (3)$$

with β_s and β_w are the thermal expansion coefficients of the solid and the water phase.

– *Energy balance equation* (for the whole system) accounting for the conductive and convective heat flow and heat effects of phase changes can be written as [7]:

$$(\rho C_p)_{eff}\frac{\partial T}{\partial t} + \left(\rho_w C_p^w \mathbf{v}^{ws} + \rho_g C_p^g \mathbf{v}^{gs}\right)\cdot grad\, T - div\left(\chi_{eff}\, grad\, T\right) = -\dot{m}_{vap}\Delta H_{vap}, \quad (4)$$

where χ_{eff} is the effective thermal conductivity, $(\rho C_p)_{eff}$ the thermal capacity of the multiphase system, ΔH_{vap} the enthalpy of water vaporization, C_p^w and C_p^g are the specific heats of the water and gas phase, while the mass source of vapour due to vaporization is determined from the water mass balance equation and takes the following form [7]:

$$\dot{m}_{vap} = \rho^w\beta_{sw}\frac{\partial T}{\partial t} - \rho^w n\frac{\partial S_w}{\partial t} - \frac{1-n}{\rho^s}\rho^w S_w\left(\frac{\partial \rho^s}{\partial \varepsilon_{ASR}^{vol}}\frac{\partial \varepsilon_{ASR}^{vol}}{\partial t} + \frac{\partial \rho^s}{\partial m_{ASR}}\dot{m}_{ASR}\right) - div\left(nS_w\rho^w\mathbf{v}^{ws}\right) - \alpha\rho^w S_w div\,\mathbf{v}^s - \dot{m}_{ASR} + \frac{\dot{m}_{ASR}}{\rho^s}\rho^w S_w. \quad (5)$$

– *Linear momentum balance equation* (for the multiphase system) in the rate form is as follows [7]:

$$div\left[\frac{\partial \mathbf{t}^{ef}}{\partial t} - \left(\frac{\partial p^g}{\partial t} - \frac{\partial x_{ASR}^{ws}}{\partial t}p^c - \chi_{ASR}^{ws}\frac{\partial p^c}{\partial t}\right)\right] + \frac{\partial \rho}{\partial t}\mathbf{g} = 0, \quad (6)$$

where χ_{ASR}^{ws} is the solid surface fraction, ρ the apparent density of the multiphase material, **g** the vector of gravity acceleration, and the effective stress tensor $\mathbf{t}^{ef}$ is discussed in the next section.

2.2. Effective stress principle

Cement based materials are multi-phase porous media, hence while analysing the stresses and strains of the material it is necessary to consider not only the action of an external load, but also the pressure exerted on the skeleton by fluids present in its voids. The total stress tensor, $\mathbf{t}^{tot}$, acting in any point of the porous medium may be split into the effective stress, $\mathbf{t}^{ef}$, which accounts for stress effects due to changes in porosity, spatial variation of porosity and the deformations of the solid matrix, and a part accounting for the solid phase pressure exerted by the pore fluids, P^s, [7],

$$\mathbf{t}^{tot} = \mathbf{t}^{ef} - \alpha P^s\mathbf{I} = \mathbf{t}^{ef} - \left(p^g - \chi_s^{ws}p^c\right)\mathbf{I}, \quad (7)$$

where **I** is the second order unit tensor, α the Biot coefficient, and χ_s^{ws} the fraction of skeleton area in contact with water.

In equation (7) capillary pressure is defined in such a way that it has physical meaning also in the hygroscopic range of moisture content, [7],

$$p^c \equiv p^g - p^w = \Pi^f - \gamma^{wg}J_{wg}^w. \quad (8)$$

In this region it takes also into account the effect of disjoining pressure, Π^f, besides the curvature and surface tension of the water/gas interface, J_{wg}^w and γ^{wg}. At higher relative humidity, in the capillary moisture range, the effect of disjoining pressure is neglected (Π^f=0).

2.3. Alkali-silica reaction evolution and strains induced by it

When we deal with ASR reaction at variable humidity and temperature, then ASR strains are not linearly proportional to the reaction advancement, in opposite to what happens during the reaction at constant hygro-thermal conditions [9]. Then, the final value of ASR strain $\varepsilon_{ASR,\infty}$ is not unique and it depends on the evolution of temperature and moisture content in the pores (see e.g. Figures 3-5). Hence, the reaction extent Γ_{ASR} is defined here according to thermodynamics of chemical reactions, see [12], similarly as by Steffens et al. [9].

The progress of ASR reaction is described by the following rate type evolution equation written in terms of the ASR reaction extent (Γ_{ASR}), which is an internal variable:

$$\frac{\partial \Gamma_{ASR}}{\partial t} = \frac{1-\Gamma_{ASR}}{t_R}, \quad (9)$$

where characteristic time of the reaction, t_R, is dependent on both the temperature and the reaction extent in the way described by the equation [1,3]:

$$t_R = \tau_R(T, S_w)\cdot\lambda(T, \Gamma_{ASR}), \quad (10)$$

with T_0 being the reference temperature and $\lambda(T, \Gamma_{ASR})$ the parameter describing effect of temperature defined in the following way:

$$\lambda(S_w, T, \Gamma_{ASR}) = \frac{1+\exp[-\tau_L(S_w,T)/\tau_r(S_w,T)]}{\Gamma_{ASR}+\exp[-\tau_L(S_w,T)/\tau_r(S_w,T)]}. \quad (11)$$

Latency time τ_L is associated with the dissolution of reactive silica from the aggregates, while reaction time τ_R with the reaction leading to the formation of the ASR gel. The abovementioned constants are affected by temperature and, as the experimental

data presented in [1] showed, the moisture content. Steffens proposed the following linear relations:

$$\tau_R(T,S_w) = \tau_{R0} \cdot \exp\left[\frac{E_R}{R}\cdot\left(\frac{1}{T}-\frac{1}{T_0}\right)\right]\cdot(A_R \cdot S_w + B_R) \quad (12a)$$

$$\tau_L(T,S_w) = \tau_{L0} \cdot \exp\left[\frac{E_L}{R}\cdot\left(\frac{1}{T}-\frac{1}{T_0}\right)\right]\cdot(A_L \cdot S_w + B_L) \quad (12b)$$

where S_w is the saturation degree of pores with liquid water, τ_{R0} and τ_{L0} are the values at the reference temperature T_0, the material parameters are A_R, B_R, A_L and B_L which should be determined experimentally, R – universal gas constant, while E_L and E_R are the activation energies for latency and reaction, respectively. According to [3], $E_L/R = 9400 \pm 500$ [K] and $E_R/R = 5400 \pm 500$ [K]. However, during the model calibration (section 4) by comparison with the experimental data [1, 2], application of these values did not result in a good agreement with the data. Therefore, the other activation energy values have been found.

Following [1] and [3], the expansions arising as a result of the ASR are considered as imposed strains. At constant temperature and humidity they are directly proportional to the reaction extent [1, 3]:

$$\boldsymbol{\varepsilon}_{ASR}(t) = \beta_{ASR} \cdot \Gamma_{ASR}(t)\mathbf{I}, \quad (13)$$

where $\beta_{ASR} = \varepsilon_{ASR,\infty}/3$ is the asymptotic linear expansion due to ASR for a material in a stress free state and $\mathbf{I}$ denotes the unit tensor of the second order. Parameter β_{ASR} is moisture dependent, according to the following exponential relation [9]:

$$\beta_{ASR}(S_w) = \beta_{ASR0}(S_w)^{C_{ASR}}, \quad (14)$$

where C_{ASR} is the material parameter obtained experimentally.

Larive's experiments [1] show that due to some intrinsic physicochemical processes a loss of swelling potential of already formed gel is observed. The process can be considered as a material ageing, see e.g. [9]. Taking into account this effect on the evolution of ASR strains, Steffens et al. [9] proposed an additional material parameter, called the characteristic time of ageing t_a, affecting both the ASR expansion rate and the final, asymptotic value of the ASR strains. This parameter characterizes the water-combination process of the already formed gel due to ASR reaction. Steffens et al. [9] proposed a kinetic law for the ageing in an analogous way to the first order chemical reaction:

$$\frac{\partial \Gamma_a}{\partial t} = \frac{1-\Gamma_a}{t_a}, \quad (15)$$

where Γ_a is the ageing reaction extent and t_a the ageing time.

Therefore, the ASR strain evolution law (13) for the case of variable hygro-thermal conditions can be rewritten in the following form [8]:

$$\dot{\boldsymbol{\varepsilon}}_{ASR}(t) = \frac{\alpha}{\rho^{ASR}}\cdot\dot{m}_{ASR}(t)\mathbf{I} = \frac{\alpha}{\rho^{ASR}}M(S_w)(1-\Gamma_a)\dot{\Gamma}_{ASR}\mathbf{I} \quad (16)$$

where α is chemo-elastic dilatation coefficient, ρ^{ASR} the density of gel formed, $M_{ASR}(S_w)$ means the water combination coefficient at water saturation degree S_w, describing the unit water-combination capacity of amorphous gel without ageing. $M_{ASR}(S_w)$ may be described by the following relation [9]:

$$M_{ASR}(S_w) = M_{ASR,0}\cdot\exp\left(\tilde{C}_{ASR}\cdot S_w + \tilde{D}_{ASR}\right), \quad (17)$$

with $\tilde{C}_{ASR}$ and $\tilde{D}_{ASR}$ being the material parameters, $M_{ASR,0} \equiv M_{ASR}(S_w = 1)$.

For constant temperature and humidity, Steffens et al. [9] obtained the following relation:

$$1-\Gamma_a = (1-\Gamma_{ASR})^{\beta}, \quad \text{with } \beta = t_R/t_a. \quad (18)$$

We assume that relation (18) is also valid in variable conditions and the coefficient β is not affected by humidity and temperature. This allows us writing the ASR strain evolution law (16) in the following rate form:

$$\frac{\partial \boldsymbol{\varepsilon}_{ASR}}{\partial t} = \tilde{\beta}_{ASR}(S_w)\cdot(1-\Gamma_{ASR})^{\beta}\cdot\frac{\partial \Gamma_{ASR}}{\partial t}\mathbf{I}, \quad (19)$$

where $\tilde{\beta}_{ASR}(S_w) = \frac{\alpha}{\rho^{ASR}}M_{ASR}(S_w)$ is a material function, parameters of which should be determined experimentally.

Considering that ASR is irreversible, i.e $\dot{\Gamma}_{ASR} \geq 0$ it is obvious from (16) that the ASR induced expansive strains cannot decrease. However, during the experiments concerning the evolution of ASR expansion of concrete specimens exposed to variable ambient humidity conditions Poyet [2] observed that during drying the total specimen strains were rapidly decreasing, and during rewetting they were increasing again (see Fig. 5). These phenomena are modelled here using the effective stress principle (see section 2.2), i.e. they are treated as "normal" elastic strains of already formed gel due to a change of the capillary pressure value: shrinkage strains during material drying, $\dot{S}_w < 0$, or swelling ones during mate-

rial wetting, $\dot{S}_w > 0$ (see Fig. 7). Hence, in the proposed mathematical model no change of the ASR strain of already formed gel is caused by a change of the saturation degree value [8], as can be for example observed in Fig. 7.

2.4. Constitutive relationships

In our model we assume that during the second stage of the ASR certain amount of pore water is combined with the products of the first stage of the reaction, what produces an amorphous gel in pores and causes expansion strains of a cement based material, thereupon the mass of solid skeleton gradually increases (see section 2). In stress free state and homogeneous, constant hygro-thermal conditions, the volume of skeleton and that of the pores increase to the similar extent, i.e. $\left[1+\varepsilon_{ASR}^{vol}(t)\right]$ – times (assuming that volume of arising micro-cracks is negligibly small), thus one observes almost no variation of the total material porosity, $n \simeq \text{const.}$ $\varepsilon_{ASR}^{vol}(t) = \text{tr}\,\boldsymbol{\varepsilon}_{ASR}(t)$ is the actual value of volumetric strain due to ASR.

The only result of the ASR is an alteration of its inner structure (finer pores volume increases), hence it causes changes of the sorption isotherm and material permeability.

Density of the ASR reacted material is defined by the following relation:

$$\rho^{s}(t) = \frac{\rho^{s0} + m_{ASR}(t)(1-n)^{-1}}{1+\varepsilon_{ASR}^{vol}(t)}, \qquad (20)$$

where ρ^{s0} means the density of unreacted skeleton.

The values of $m_{ASR}(t) = \dfrac{\rho^{ASR}}{\alpha}\,\text{tr}\,\boldsymbol{\varepsilon}_{ASR}(t)$ and ε_{ASR}^{vol} are obtained by numerical integration in time of equation (19).

During evolution of the ASR, porosity of damaged material, n, remains constant, but due to the reaction induced increase of the material total volume,

$$V_{tot}(t) = V_{tot}(t=0)\left[1+\text{tr}\,\boldsymbol{\varepsilon}_{ASR}(t)\right], \qquad (21)$$

the pore volume increases $[1+\varepsilon_{ASR}^{vol}(t)]$- times causing a decrease of the water saturation degree S_w (assuming that volume of arising micro-cracks is negligibly small).

It is assumed that variation of the material microstructure due to ASR can be described by evolution of the material sorption isotherms. An "intermediate" sorption curve between those of the unreacted and fully ASR reacted material is proportional to the actual volume of produced gel. The volume is approximately proportional to the mass of water m_{ASR} combined with the gel during the second stage of the ASR reaction. Hence, the following equation describing evolution of the sorption isotherms during ASR is proposed [8]:

$$S_w(p^c, m_{ASR}) = S_w(p^c, 0) + \frac{m_{ASR}}{m_{ASR,\infty}}\left[S_w(p^c, m_{ASR,\infty}) - S_w(p^c, 0)\right] \qquad (22)$$

where $S_w(p^c, m_{ASR,\infty})$ and $S_w(p^c, 0)$ are the sorption isotherms of fully ASR reacted and unreacted material, accordingly, and $m_{ASR,\infty}$ is the final mass of combined water during gel formation in a material fully saturated with water during the whole ASR, i.e. in conditions when the ASR strain is the largest. Dependence of the sorption isotherms on the temperature can be neglected for the range of temperature analysed here.

Effect of the ASR reaction on the material intrinsic permeability is described here similarly as that caused by hydration of cement based materials, which also results in a gradual development of finer pore structure [7]. The hydration degree in the aforementioned relation will be substituted with $m_{ASR}/m_{ASR,\infty}$, describing a relative increase of the ASR gel pores' volume. Then, cracking of concrete due to an external load and/or an increase of the effective skeleton stresses (e.g. during material drying), causes an additional increase of the intrinsic permeability k which may be described through its dependence upon the mechanical damage, d (see eq. 26), similarly as in [13]. Finally, we have assumed that the two aforementioned effects are independent one upon another and taken into account by the following equation:

$$k = k(m_{ASR}, d) = k_o \cdot 10^{A_k\left(m_{ASR}/m_{ASR,\infty}\right)} \cdot 10^{A_d d}, \qquad (23)$$

where k_o means the intrinsic permeability of ASR unreacted material, A_k and A_d are the experimentally determined material parameters. The value of the A_k parameter is equal to $\log(k_{ASR,\infty}/k_o)$, where $k_{ASR,\infty}$ is the final value of experimentally determined intrinsic permeability of mechanically undamaged (uncracked) material, fully saturated with water during the whole ASR reaction. The value of the A_d parameter is equal to $\log[k(m_{ASR,\infty}=0,\ d=1)/k_o]$, where $k(m_{ASR,\infty}=0,\ d=1)$ is the value for unreacted ($\Gamma_{ASR}=0$), but fully mechanically damaged ($d=1$) material.

Assuming infinitesimal deformations, the constitutive relationship, describing the stress-strain behav-

iour of concrete deteriorated by the ASR at non-isothermal conditions, takes the following form,

$$\dot{\mathbf{t}}^{ef} = \mathbf{D}\left(\dot{\boldsymbol{\varepsilon}}_{tot} - \dot{\boldsymbol{\varepsilon}}_c - \dot{\boldsymbol{\varepsilon}}_t - \dot{\boldsymbol{\varepsilon}}_{ASR}\right) + \dot{\mathbf{D}}\left(\boldsymbol{\varepsilon}_{tot} - \boldsymbol{\varepsilon}_c - \boldsymbol{\varepsilon}_t - \boldsymbol{\varepsilon}_{ASR}\right), \quad (24)$$

where $\mathbf{D}$ is the tangent matrix, while $\boldsymbol{\varepsilon}_{tot}$, $\boldsymbol{\varepsilon}_c$ and $\boldsymbol{\varepsilon}_t$ are the tensors of total-, creep- and thermal strain, accordingly.

The total damage parameter D is defined by the following equation,

$$1 - D = (1 - d)(1 - V), \quad (25)$$

where d is the mechanical damage parameter, and V the chemical damage parameter induced by the ASR.

Concrete cracking due to external load and internal one (i.e. solid pressure, see section 2.2) is modelled by means of the non-local isotropic damage theory [14]. Advancement of material cracking is described by the mechanical damage variable d, which is defined as, [14] :

$$d = 1 - \frac{E}{E_0}, \quad (26)$$

where E_0 is the Young's modulus of elasticity for a sound material (ε_{ASR}^{vol}=0, d=0), and E – for mechanically degraded material due to cracking.

Additionally, to take into account the effects of micro-cracking processes due to degradation of concrete strength properties caused by the ASR, a scalar chemical damage parameter, V, is applied, similarly to what was done in [13] for concrete at high temperature, and in [15] for concrete exposed to calcium leaching. Here chemical damage parameter is defined as follows,

$$V = 1 - \frac{E\left(\varepsilon_{ASR}^{vol}, 0\right)}{E_0}, \quad (27)$$

where $E\,(\varepsilon_{ASR}^{vol}, 0)$ is the Young's modulus of elasticity for the material deteriorated chemically due to ASR, but with no mechanical damage (d= 0). Some experimental data concerning cement composites, e.g. [16, 17], show that process of chemical deterioration due to ASR for this material starts above certain threshold volumetric strain $\varepsilon_{ASR,lim}^{vol}$. For the cement mortars tested in [16] this threshold value was equal to $\varepsilon_{ASR,lim}^{vol} \approx 0.8‰ \div 1.0‰$, and the maximal value of chemical damage parameter $V_{max} \approx 0.15 \div 0.2$, as can be seen in Fig. 1. From Fig. 1 it is clear, that the relation $V(\varepsilon_{ASR}^{vol})$ can be approximately described by means of a linear function of the following form,

$$V\left(\varepsilon_{ASR}^{vol}\right) = 0; \qquad \text{for } \varepsilon_{ASR}^{vol} \le \varepsilon_{ASR,\lim}^{vol},$$

$$V\left(\varepsilon_{ASR}^{vol}\right) = \frac{V_{\max}}{\varepsilon_{ASR,\max}^{vol} - \varepsilon_{ASR,\lim}^{vol}}\left(\varepsilon_{ASR}^{vol} - \varepsilon_{ASR,\lim}^{vol}\right) \quad \text{for } \varepsilon_{ASR}^{vol} \le \varepsilon_{ASR,\lim}^{vol}, \quad (28)$$

where $\varepsilon_{ASR,\max}^{vol}$ means the maximum value of volumetric strain due to ASR in a material fully saturated with water (S_w= 1).

For concrete a linear relationship also holds, but with slightly higher maximal value of chemical damage parameter V_{max}, which reaches values up to 0.3÷0.4 [17].

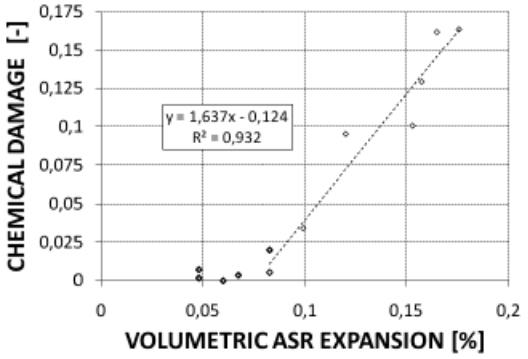

Figure 1.
Dependence of the chemical damage parameter upon the volumetric expansion for a cement mortars deteriorated due to the ASR, determined using the experimental data from [16]

3. NUMERICAL MODEL

The model equations are discretized in space by means of the finite element method. The unknown variables are expressed in terms of their nodal values and shape functions $\mathbf{N}_\kappa$ ($\kappa = g, c, t, u$) as

$$p^g(t) \cong \mathbf{N}_p \bar{\mathbf{p}}^g(t), \quad p^c(t) \cong \mathbf{N}_p \bar{\mathbf{p}}^c(t), \quad T(t) \cong \mathbf{N}_t \bar{\mathbf{T}}(t), \quad \mathbf{u}(t) \cong \mathbf{N}_u \bar{\mathbf{u}}(t). \quad (29)$$

The discretized form of the model equations was obtained by means of Galerkin's method, similarly as done for maturing concrete by Gawin et al. [7]. The equations can be written in the following concise matrix form:

$$\mathbf{C}_{ij}(\mathbf{x})\frac{\partial \mathbf{x}}{\partial t} + \mathbf{K}_{ij}(\mathbf{x})\,\mathbf{x} = \mathbf{f}_i(\mathbf{x}), \qquad \mathbf{x} = \left\{\bar{\mathbf{p}}^g, \bar{\mathbf{p}}^c, \bar{\mathbf{T}}, \bar{\mathbf{u}}\right\}^T, \quad (30)$$

where the non-linear matrix coefficients $\mathbf{C}_{ij}(\mathbf{x})$, $\mathbf{K}_{ij}(\mathbf{x})$ and $\mathbf{f}_i(\mathbf{x})$ are defined in detail in [8]. The time discretization is accomplished through a fully implicit finite difference scheme,

$$\boldsymbol{\Psi}^i(\mathbf{x}_{n+1}) = \mathbf{C}_{ij}(\mathbf{x}_{n+1})\frac{\mathbf{x}_{n+1} - \mathbf{x}_n}{\Delta t} + \mathbf{K}_{ij}(\mathbf{x}_{n+1})\,\mathbf{x}_{n+1} - \mathbf{f}_i(\mathbf{x}_{n+1}) = \mathbf{0}, \qquad (i = g, c, t, u) \quad (31)$$

where n is the time step number and Δt the time step length.

The equation set (31) is solved by means of a monolithic Newton-Raphson type iterative procedure using a frontal solver, [7, 13].

The reaction extent and mass of combined water by the ASR gel at $(n+1)$ time step and $(k+1)$ iteration, $(\Gamma_{ASR})_{n+1}^{k+1}$ and, $(m_{ASR})_{n+1}^{k+1}$ are calculated separately using the implicit Euler method:

$$(\Gamma_{ASR})_{n+1}^{k+1} = (\Gamma_{ASR})_n + \frac{1-(\Gamma_{ASR})_{n+1}^{k}}{(t_R)_{n+1}^{k}}\Delta t, \qquad (32)$$

$$(m_{ASR})_{n+1}^{k+1} = (m_{ASR})_n + (\dot{m}_{ASR})_{n+1}^{k}\Delta t. \qquad (33)$$

4. NUMERICAL EXAMPLES

The following three problems, based on the laboratory tests performed by Larive [1] and Poyet [2], are numerically solved in order to validate the present model by comparison with the experimental results. The simulations were performed by means of the computer code developed by the Authors on basis of the finite element model of concrete COMES-GEO [7], which was appropriately modified in order to take into consideration ASR.

Table 1.
Material parameters assumed in the simulations of Larive's and Poyet's experiment

Material parameter	Larive test	Poyet test
Water / cement ratio, w/c [-]	0.48	0.50
Initial value of the latency time, τ_{L0} [days]	40.1	37.0
Initial value of the reaction time, τ_{R0} [days]	16.9	67.0
Activation energy for the latency, E_L/R [K]	6000	10000
Activation energy for the reaction, E_R/R [K]	2500	6000
Coeff. for the water content dependency in the latency period, A_L [-]	-8.7	-1.0
Coeff. for the water content dependency in the latency period, B_L [-]	9.7	2.0
Coeff. for the water content dependency during the reaction, A_R [-]	-6.94	-1.00
Coeff. for the water content dependency during the reaction, B_R [-]	7.94	2.00
Ageing time, τ_A [days]	145.3	200.0
Coeff. for the β function in the ASR strain rate formula, $\tilde{\beta}_{ASR}$ [-]	0.0037	0.0043
Coeff. for the β function in the ASR strain rate formula, $\tilde{C}_{ASR0}$ [-]	3.56	1.10
Porosity, n [%]	10	17
Intrinsic permeability of unreacted material, k_0 [m^2]	$0.5\cdot10^{-19}$	$0.5\cdot10^{-20}$

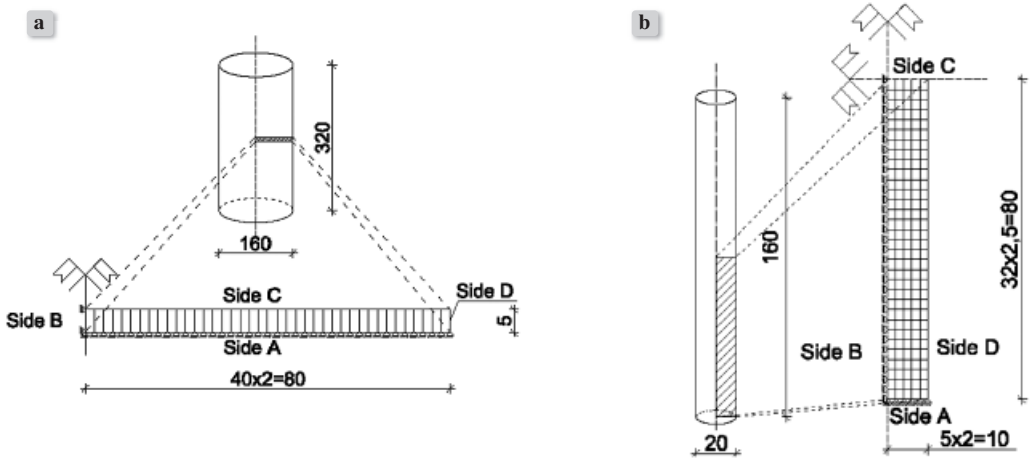

Figure 2.
FE mesh assumed in the simulations of Larive's (a) and Poyet's (b) experiments

4.1. Larive's experiment

The laboratory tests by Larive [1] took particular interest in influence of water content and temperature on ASR. The cylindrical specimens (16cm in radius, 32cm in height) were exposed to various thermal and hygral conditions. After casting and curing they were either kept in ambient humidity and three different temperatures: 296.15K, 311.15K and 333.15K (23°C, 38°C and 60°C), or at temperature of 311.15 K (38°C) and constant relative humidity levels corresponding to the water saturation degrees S_w equal to 73%, 87.5%, 92.5% and 100% (in water). More details about this experiment can be found in [1].

The main parameters defining physical properties of the material assumed in the simulations are summarized in Table 1. Due to lack of sufficient material data, chemical damage was not considered in the computations. The specimens were modelled with the mesh of 40 (40 x 1) 8-noded finite elements of equal size (2mm x 5mm), Fig. 2a. Convective boundary conditions for heat and water exchange were assumed at the external specimen surface (side D in Fig. 2a). The time step length increasing from 1 hour up to 1 day, depending on the stage of the process evolution, was used in the computations.

As can be noticed (Fig. 3), the results obtained by means of the simulations are in a good agreement with the experimental data. The presented model reflects influence of temperature and relative humidity on the final values and development of strains caused by ASR.

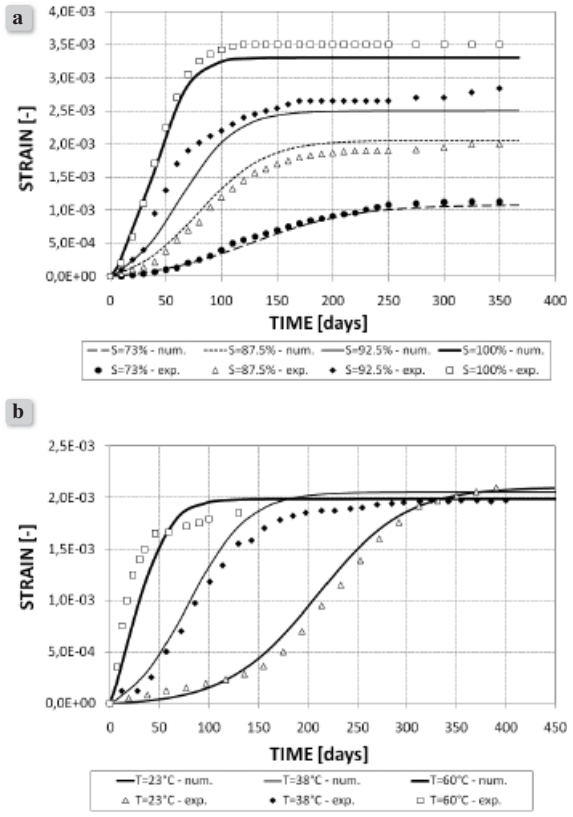

Figure 3.
Comparison of the experimental [1] and numerical results of ASR expansion for the specimens stored in different relative humidity (a) and temperature (b)

4.2. Poyet's experiment

The experiments conducted by Poyet [2] were simulated in order to check the capability of the model to predict strains caused by ASR in various relative humidity conditions. Two series of tests were performed. In the first series, after maturing at 82 %RH, the specimens were exposed to ambient air with constant relative humidity, which was kept at six different levels: 59, 76, 80, 82, 96 and 100 [%RH]. For all the considered cases air temperature was kept constant at 333.15 K (60°C). We focus our attention on the results for four levels of RH only, omitting those concerning 80%RH (it is very close to the reference relative humidity chosen by Poyet as equal to 82%RH) and 100%RH (the strains measured for that case were considerably smaller than those for 96%RH, probably due to some problems during the measurements [2]).

In the second series of experiments relative humidity was cyclically changed between the two levels: 96%RH and 59%RH, either in 14-days (short) or 28-days (long) cycles (at the beginning the specimens were kept at 96%RH for 3 days and later moved to 59%RH, then to 96%RH, etc.). All the time the air temperature was kept constant at 333.15 K (60°C).

Calculations were made for one fourth of the specimen cross-section, modelled with 160 (5 x 32) 8-noded (2 mm x 2.5 mm) finite elements (see Fig. 2b). The main material parameters assumed for concrete in the simulations are given in Table 1. Due to lack of sufficient material data, chemical damage was not considered in the computations.

Convective boundary conditions for heat and water exchange were assumed at the external specimen surfaces (sides C and D in Fig. 2b). For the cases with constant ambient humidity, the increasing time step length, from 3 s up to 80 min, was used in the computations. For the cases with cyclically changing ambient humidity, the variable time step length, from 3 s to 30 s, depending on the stage of the process evolution, was applied.

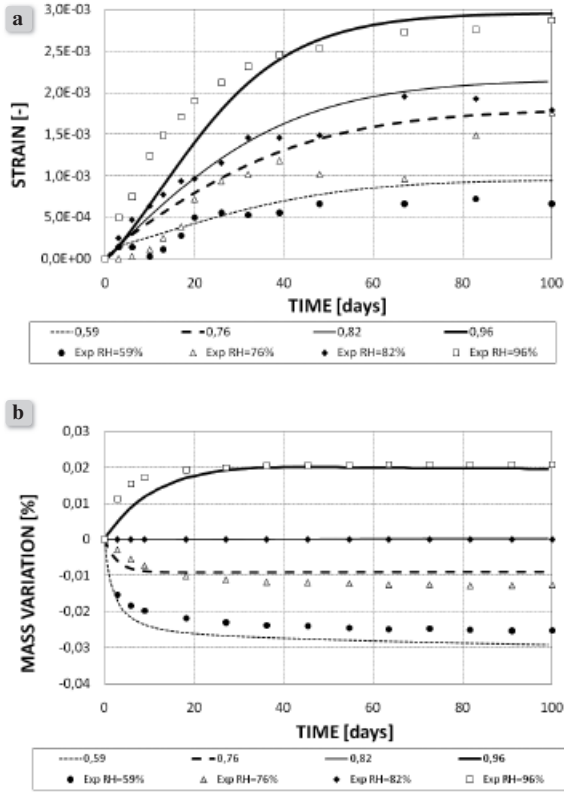

Figure 4.
Comparison of the experimental and numerical results for the ASR expansion strains (a) and water mass variation (b) at three constant relative humidity levels

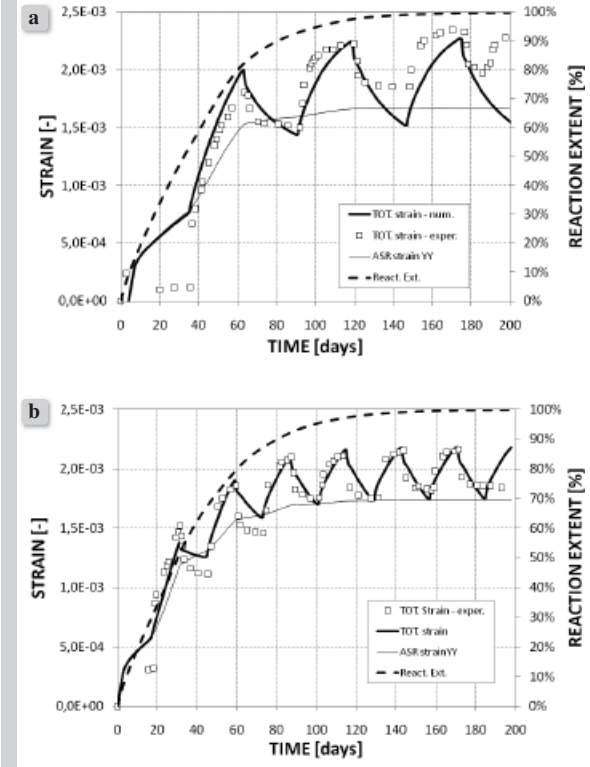

Figure 5.
Comparison of the experimental and numerical results for the variation of ASR expansion strains at variable relative humidity for the long (a) and short (b) cycles. Additionally, the temporal evolutions of ASR reaction extent and ASR strain are presented

The ASR expansion strains, both during the experiments and the simulations, were determined with respect to the reference specimen, made of nonreactive aggregate and exposed to the same hygro-thermal conditions as the considered one. As can be seen in Figures 4-6, the set of parameters calibrated for the series at constant relative humidity assured a good agreement for the series at variable humidity as well. For the latter series the ASR strains agreement with the experimental data (Fig. 5) is better than for the mass variation (Fig. 6), what was caused by lack of several moisture related material parameters. At the latter conditions, the agreement for the ASR strains (Fig. 5) is visibly better than for the mass variation (Fig. 6), what was caused by lack of most of the moisture related material parameters, hence some of them were assumed from literature [18]. Part of material parameters, describing changes of inner structure and related physical properties (sorption isotherm, intrinsic permeability, solid surface fraction) due to ASR, were determined by means of the inverse solution technique. Additionally, the temporal evolutions of ASR reaction extent and ASR strains are presented in Fig. 5, showing a considerable effect of relative humidity on their development.

Figure 7 shows the temporal evolutions of different components of concrete strains for the series with long cycle variation of relative humidity. As can be observed, the ASR strain is always monotonically increasing, while the oscillations of total strain are caused by changes of shrinkage strain, following variations of the material relative humidity.

In Fig. 8 one can notice the effect already mentioned in [2], i.e. during cyclically variable relative humidity ASR expansion does not reach the same final value as in the conditions of constant relative humidity. According to the laboratory tests data, the final values of strain at constant environmental conditions are approximately equal to 0.28% for 96%RH and 0.07% for 59%RH, while in the case of variable relative humidity those strains are equal to about 0.21% and 0.18%, respectively. Similar effect can be observed for the numerical results, see Fig. 8. The variation of ASR strains at different stages of the

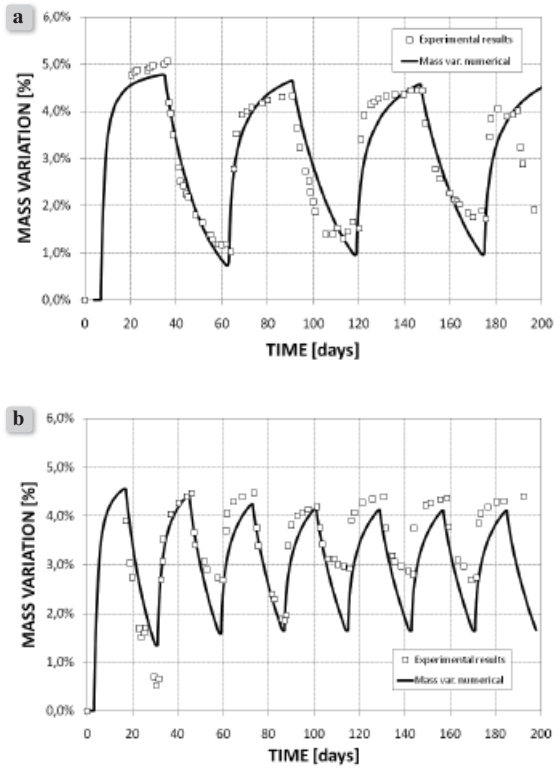

Figure 6.
Comparison of the experimental and numerical results for the variation of mass of water at variable relative humidity for the long (a) and short (b) cycles

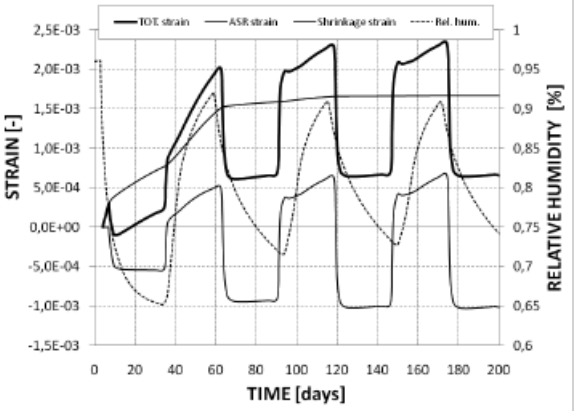

Figure 7.
Numerical results for the temporal evolution of different components of strains at variable relative humidity for the long cycle. Additionally variations of the relative humidity are shown

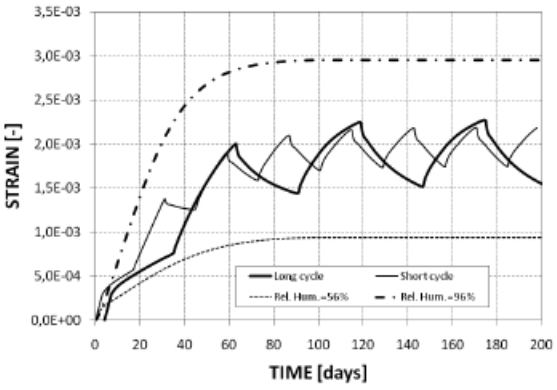

Figure 8.
Comparison of the numerical results concerning the temporal evolution of the ASR expansion development for constant and variable relative humidity

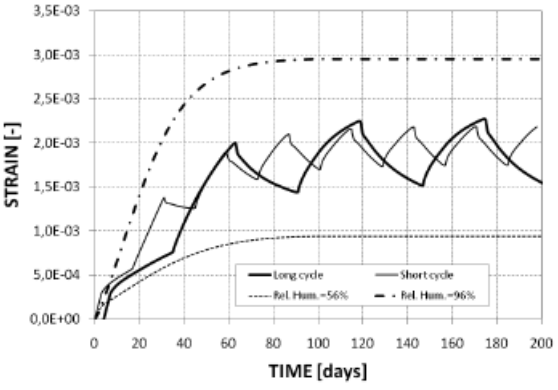

Figure 9.
Comparison of the numerical results concerning the evolution of ASR expansion in function of the reaction extent for constant and variable relative humidity

reaction advancement, for all analysed cases of constant and variable relative humidity, are shown in Fig. 9. One can observe that variable hygral conditions have a small influence on the progress of ASR reaction (compare Figures 5a and 5b) and quite significant effect on the concrete strains due to the ASR at all stages of the reaction development, in particular at the advanced ones, Fig. 9.

5. CONCLUSIONS

A novel mathematical model of hygro-thermal behaviour of cement based materials subjected to the degradation due to ASR has been presented. The reaction has been described by a rate type model. Thanks to that it is possible to take into account the influence of variable moisture content and temperature upon the development of ASR. The model is thermo-dynamically consistent and it has been developed within framework of mechanics of multi-phase porous media. The experimental studies of ASR indicate a considerable effect of the concrete temperature and moisture state on the evolution of the material strains, what is properly described by the proposed model. The simulation results show that the present model allows for prediction of a cement-based material performance, and in particular, strains evolution, with a reasonable accuracy. Further developments of the model to take into account effect of external load and the ASR strains anisotropy are in progress.

ACKNOWLEDGEMENTS

The scientific research reported here has been carried out as a part of the Project "Innovative recourses and effective methods of safety improvement and durability of buildings and transport infrastructure in the sustainable development" at the Technical University of Łódź, Poland, financed by the European Union from the European Fund of Regional Development based on the *Operational Program of the Innovative Economy*. The first and fourth authors' research was partially funded by the Research Project Ex60% – Anno: 2011 – prot. 60A09-1382/11 "Modellazione matematico-numerica dei fenomeni di deterioramento chemo-fisico-meccanico nei materiali cementizi" financed by the University of Padova, Italy.

REFERENCES

[1] *Larive C.*; Apport combinés de l'alcali-réaction et des ses effets mecaniques. PhD Thesis, Ecole Nationale des Ponts et Chaussées, Marne-la-Vallée, 1997

[2] *Poyet S.*; Etude de la dégradation des ouvrages en béton atteints de la réaction alcali-silice: approche expérimentale et modélisation numérique multi-échelle des dégradations dans un environnement hydro-chemo-mécanique variable. PhD Thesis, University of Marne la Vallée, France, 2003

[3] *Ulm F.J., Coussy O., Kefei L., Larive C.*; Thermo-chemo-mechanics of ASR expansion in concrete structures. J. of Engineering Mechanics, Vol.126, No.3, 2000; p.233-242

[4] *Multon S., Toutlemonde F.*; Effect of applied stresses on alkali-silica reaction-induced expansions. Cement and Concrete Research, Vol.36, 2006; p.912-920

[5] *Winnicki A., Pietruszczak S.*; On mechanical degradation of reinforced concrete affected by alkali-silica reaction. J. of Engineering Mechanics, Vol.134, No.8, 2008; p.611-62

[6] *Torrijos M. C., Giaccio G., Zerbino R.*; Internal cracking and transport properties in damaged concretes. Materials and Structures, Vol.43, 2010; p.109-121

[7] *Gawin D., Pesavento F., Screfler B.A.*; Hygro-thermo-chemo-mechanical modelling of concrete at early ages and beyond. Part I: Hydration and hygro-thermal phenomena. Int. J. for Numerical Methods in Engineering, Vol.67, 2006; p.299-331

[8] *Pesavento F., Gawin D., Wyrzykowski M., Simoni L.*; Modelling alkali-silica reaction in non-isothermal, partially saturated cement based materials. Submitted for publication

[9] *Steffens A., Li K., Coussy O.*; Ageing approach to water effect on alkali-silica reaction. Degradation of structures. J. of Engineering Mechanics, Vol.129, No.1, 2003; p.50-59

[10] *Bangert F., Kuhl D., Meschke G.*; Chemo-hygro-mechanical modeling and numerical simulation of concrete deterioration caused by alkali-silica reaction. Int. J. for Numerical and Analytical Methods in Geomechanics, Vol.28, 2004; p.689-714

[11] *Baroghel-Bouny V., Mainguy M., Lassabatere T., Coussy O.*; Characterization and identification of equilibrium and transfer moisture properties for ordinary and high-performance cementitious materials. Cement and Concrete Research, Vol.29, 1999; p.1225-1238

[12] *Aitkins P., De Paula J.*; Aitkins' Physical Chemistry, Seventh Edition. Oxford University Press Inc., New York, 2002.

[13] *Gawin D., Pesavento F., Schrefler B.A.*; Modelling of hygro-thermal behaviour of concrete at high temperature with thermo-chemical and mechanical material degradation. Computer Methods in Applied Mechanics and Engineering, Vol.192, 2003; p.1731-1771

[14] *Mazars J., Pijaudier-Cabot J.*; Continuum damage theory – application to concrete. Journal of Engineering Mechanics ASCE, Vol.115, No.2, 1989; p.345-365

[15] *Gawin D., Pesavento F., Schrefler B.A.*; Modeling deterioration of cementitious materials exposed to calcium leaching in non-isothermal conditions. Computer Methods in Applied Mechanics and Engineering, Vol.198, 2009; p.3051-3083

[16] *Ben Haha M.*; Mechanical effects of alkali silica reaction in concrete studied by SEM-image analysis. Ph.D. Thesis, École Polytechnique Fédérale de Lausanne EPFL, Lausanne, 2006

[17] *Dunant C.F., Scrivener K.L.*; Micro-Mechanical Modelling of Alkali-Silica–Reaction Induced degradation using the AMIE framework. Cement and Concrete Research, Vol.40, No.4, 2010; p.517-525

[18] *Baroghel-Bouny V., Mainguy M., Lassabatere T., Coussy O.*; Characterization and identification of equilibrium and transfer moisture properties for ordinary and high-performance cementitious materials. Cement and Concrete Research, Vol.29, 1999; p.1225-1238